

# Synthesis characterization and hydrogenation behaviour of as quenched $\text{Ti}_{41.5+x}\text{Zr}_{41.5-x}\text{Ni}_{17}$ ( $x=0, 3.5, 11.5$ and $13.5$ ) nano quasicrystalline ribbons

Rohit R Shahi<sup>1</sup>, T.P. Yadav<sup>2</sup>, M.A. Shaz<sup>2</sup>, O.N. Srivastava<sup>2</sup>

<sup>1</sup>Department of Physics Motilal Nehru National Institute of Technology Allahabad-211004 India,

<sup>2</sup>Department of Physics, Banaras Hindu University Varanasi-221005, India  
Email; [rohitrshahi@gmail.com](mailto:rohitrshahi@gmail.com)

**Abstract.** The present study describes the synthesis characterization and hydrogen storage behavior of  $\text{Ti}_{41.5+x}\text{Zr}_{41.5-x}\text{Ni}_{17}$  ( $x=0, 3.5, 11.5$  and  $13.5$ ) nano quasicrystalline ribbons synthesized through rapid solidification technique. The nano quasicrystalline ribbons of alloys have been synthesized at Cu-wheel speed of 45 m/sec. The investigation also describes the effect of different compositions of Ti and Zr on the structure, microstructure and their correlation with hydrogen storage characteristics of as quenched nano quasicrystalline ribbons. It has been found that the hydrogen storage capacity of these ribbons increases with increasing the content of Ti in i-phase ribbons.

## 1. Introduction

It is now well known that storage of hydrogen is main challenge in developing hydrogen economy. Hydrogen can be stored at moderate temperature and pressure in intermetallic compounds and formed metal hydrides [1, 2]. Intensive research has been conducted in last few decades on metal hydrides to improve the hydrogen storage capacity, kinetics, thermal properties and cycling behavior [3]. In this series quasicrystalline alloys have lately be confirmed to store large amount of hydrogen reversibly because of the availability of higher number of interstitial voids [4]. After the discovery of a stable icosahedral phase (i-phase) in Ti-Zr-Ni system, this system received attention as hydrogen storage materials [5, 6]. The hydrogen uptake capacity of i - phase is found to be higher as compared to other crystalline phases due the shell structure of i-phase which provide higher density of interstitial voids as compared to crystalline phases. For the Ti-Zr-Ni system the presence of Ti/Zr enhances the hydrogen uptake capacity due to the better affinity of Ti and Zr towards hydrogen. Moreover, the presence of Ni enhances the dissociation of hydrogen molecule to hydrogen atom at the surface and it often creates a pathway for H diffusion through a surface oxide layer.

Ti-based IQC alloys can be synthesized by mechanical alloying followed by annealing and also by rapid solidification technique. Several studies confirmed that the phase formation and properties of these alloys strictly affected by the processing parameter and variation of stoichiometric ratio [7,8]. We have also been investigated the effect of processing parameter by changing the quenching rate on the phase formation and hydrogen storage characteristics of  $\text{Ti}_{45}\text{Zr}_{38}\text{Ni}_{17}$  IQC ribbons synthesized through rapid solidification technique and further investigated their hydrogenation characteristics [9]. It has been found that hydrogen uptake capacity as well as the absorption kinetics of the IQC ribbons increases with increasing the quenching rate at which the ribbons were synthesized due to the



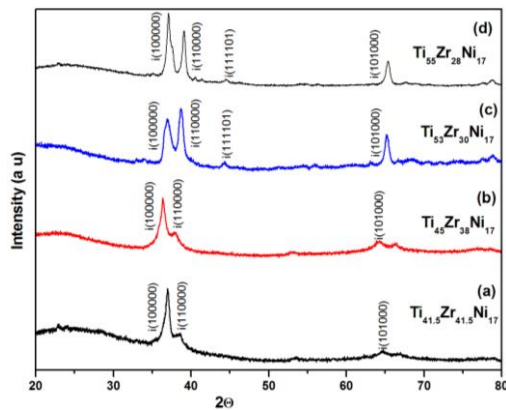
formation of nano grains of i-phase. In the present report, we have investigated the effect of composition on the phase formation, microstructure and their hydrogen storage behavior of  $\text{Ti}_{41.5+x}\text{Zr}_{41.5-x}\text{Ni}_{17}$  ( $x= 0, 3.5, 11.5$  and  $13.5$ ) i-phase ribbons. We have synthesized nano quasicrystalline ribbons of  $\text{Ti}_{41.5+x}\text{Zr}_{41.5-x}\text{Ni}_{17}$  at wheel speed of 45m/s and investigated their hydrogen storage characteristics.

## 2. Experimental Details

Alloy ingots of desired stoichiometry were prepared by RF induction melting of pure Ti (99.99%), Zr (99.99%) and Ni (99.99%) metal in graphite crucible under argon atmosphere. About 10g as cast ingots were melted 4 times to achieve chemical homogeneity. Further the alloy ingot was subjected to rapid solidify by using Cu-wheel of diameter 14 cm and at tangential speed of 45m/s . The formed ribbons have the thickness of 40 to 50  $\mu\text{m}$  and length 30 to 40 cm. The synthesized ribbons were structurally characterized by X-ray diffraction (XRD) (Rigaku) equipped with  $\text{CuK}\alpha$  radiation. The XRD data is further used to evaluate the lattice strain and crystallite size of the synthesized ribbon through pseudo Viot function analysis [10]. The microstructure and rotational symmetry of the synthesized ribbons were investigated through transmission electron microscopy (TEM) (FEI-Tecnai 20 G<sup>2</sup>). The TEM sample were prepared by thinning of ribbons through an electro-polishing unit (Tenupol-5) using electrolyte 1:4 ratios of  $\text{HClO}_4$  and methanol at 30°C. The surface morphology and composition of the synthesized ribbons were characterized by scanning electron microscopy (SEM) (Quanta 200) equipped with EDAX facility. The hydrogen sorption behavior was examined through the computerized pressure-concentration-temperature measurement system (AMC-USA) having the facility to measured the absorption desorption kinetics of the samples.

## 3. Results and Discussion

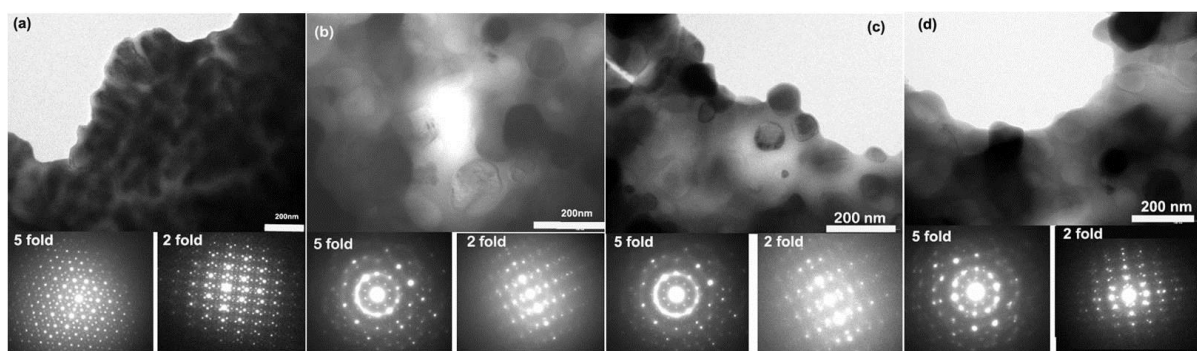
We have already investigated the effect of quenching rate on phase formation and hydrogen storage behavior of  $\text{Ti}_{45}\text{Zr}_{38}\text{Ni}_{17}$  IQC ribbons and found that 45m/s wheel speed is sufficient for the synthesis of nano quasicrystalline phase [7]. Therefore, in the present study we have synthesized ribbons of  $\text{Ti}_{41.5+x}\text{Zr}_{41.5-x}\text{Ni}_{17}$  ( $x=0, 3.5, 11.5$  and  $13.5$ ) at wheel speed of 45m/s. Fig. 1 represents XRD patterns of different  $\text{Ti}_{41.5+x}\text{Zr}_{41.5-x}\text{Ni}_{17}$  ribbons (for  $x=0, 3.5, 11.5$  and  $13.5$ ) at wheel speed of 45m/s. A hump like region appeared in all the XRD patterns which are coming from the XRD sample holder. The XRD pattern of  $\text{Ti}_{41.5}\text{Zr}_{41.5}\text{Ni}_{17}$  (as shown in fig 1(a)) having peaks index with i-phase (indexed according Bancel scheme [11]). Further if we increase the content of Ti from 41.5 to 45 at% and correspondingly decrease the content of Zr from 41.5 to 38 at% the XRD pattern of  $\text{Ti}_{45}\text{Zr}_{38}\text{Ni}_{17}$  ribbons reveals the presence of peaks which are indexed with i-phase similar to the case of  $\text{Ti}_{41.5}\text{Zr}_{41.5}\text{Ni}_{17}$ . However, the peak of i-phase becomes broadened as compared to first sample and shifted towards lower  $2\theta$  values from 36.93 to 36.37 for  $\text{Ti}_{45}\text{Zr}_{38}\text{Ni}_{17}$ . As we further increase the content of Ti from 45 to 53 ( $x=11.5$ ) the peaks correspond to i-phase become broadened and shifted towards higher  $2\theta$  values (as shown in fig 1(c)). This may happen due to higher concentration of Ti and lower concentration of Zr. Further by increasing the content of Ti (from 53 to 55 at %) ( $x=13.5$ ) and correspondingly decrease the content of Zr the position of most intense peak is same as that of the case for  $\text{Ti}_{53}\text{Zr}_{30}\text{Ni}_{17}$  (as shown in fig. 1(d)). In order to understand the effect of different concentration of Ti and Zr on crystallite size and lattice strain, we have evaluated these by pseudo Viot function analysis of XRD profile. In this regard, the most intense peak of i-phase has been fitted by considering Gaussian and Lorentzian profile function. The Gaussian and Lorentzian widths were separated out and as we know these are correspond to lattice strain and crystallite size respectively. The evaluated lattice strain and crystallite size for  $\text{Ti}_{41.5+x}\text{Zr}_{41.5-x}\text{Ni}_{17}$  i-phase ribbons are summarized in Table1 and found that as we increase the content of Ti, the crystallite size of the synthesized i-phase is decreased.

**Table 1; for lattice strain and crystallite size**

Sample	Lattice strain ( $\pm 0.05$ )	Crystallite Size ( $\pm 0.5$ nm) (nm)
$\text{Ti}_{41.5}\text{Zr}_{41.5}\text{Ni}_{17}$	0.185	30.7
$\text{Ti}_{45}\text{Zr}_{38}\text{Ni}_{17}$	0.261	27.5
$\text{Ti}_{53}\text{Zr}_{30}\text{Ni}_{17}$	0.310	20.0
$\text{Ti}_{55}\text{Zr}_{28}\text{Ni}_{17}$	0.210	15.7

**Fig.1** XRD patterns of (a)  $\text{Ti}_{41.5}\text{Zr}_{41.5}\text{Ni}_{17}$ , (b)  $\text{Ti}_{45}\text{Zr}_{38}\text{Ni}_{17}$ , (c)  $\text{Ti}_{53}\text{Zr}_{30}\text{Ni}_{17}$  and (d)  $\text{Ti}_{55}\text{Zr}_{28}\text{Ni}_{17}$  ribbon synthesized at wheel speed of 45 m/s

The TEM micrograph of  $\text{Ti}_{41.5+x}\text{Zr}_{41.5-x}\text{Ni}_{17}$  ( $x=0, 3.5, 11.5$  and  $13.5$ ) i-phase ribbons synthesized at 45m/s are shown in Fig.2. Fig.2 (a) represents the TEM micrograph of  $\text{Ti}_{41.5}\text{Zr}_{41.5}\text{Ni}_{17}$  ribbon reveals the formation grains of size 200 nm. The corresponding SAED patterns show the characteristics 5-fold and 2-fold symmetry of i-phase at different tilt (shown in fig. 2(a)). The synthesized ribbon of  $\text{Ti}_{45}\text{Zr}_{38}\text{Ni}_{17}$  having grains ranges from 100–150 nm (as shown in Fig. 2b). The corresponding SAED pattern at different tilt shows the 5-fold and 2-fold symmetry of i-phase. Fig.2(c) represents the TEM micrograph of  $\text{Ti}_{53}\text{Zr}_{30}\text{Ni}_{17}$  ribbon reveals the formation of i-phase grains of size ranges from 20-50 nm. The representative SAED pattern reveals diffuse ring along with the distorted 5-fold symmetry which is appearing due to the formation of nano grains. For the case of  $\text{Ti}_{55}\text{Zr}_{28}\text{Ni}_{17}$  the microstructure remains the similar as  $\text{Ti}_{53}\text{Zr}_{30}\text{Ni}_{17}$  ribbons. However, the grain size of i-phase is further decreased even by slight change of Ti content (53 to 55 at%). Hence it confirms that as we increase the content of Ti the grain size of the synthesized ribbon decreases. The corresponding SAED pattern shows more distorted 5-fold and 2-fold symmetry. The EDAX analysis were carried out over synthesized ribbons through SEM (Quanta-200) did not reveal the oxygen content (not shown here). The alloy composition has been found close to the nominal stoichiometry taken.

**Fig.2** TEM micrograph and corresponding 5-fold, 2-fold symmetry of i-phase of (a)  $\text{Ti}_{41.5}\text{Zr}_{41.5}\text{Ni}_{17}$ , (b)  $\text{Ti}_{45}\text{Zr}_{38}\text{Ni}_{17}$ , (c)  $\text{Ti}_{53}\text{Zr}_{30}\text{Ni}_{17}$  and (d)  $\text{Ti}_{55}\text{Zr}_{28}\text{Ni}_{17}$  ribbons.

The ribbons kept in reactor were evacuated up to  $10^{-3}$  torr through vacuum pump and then heated up to  $320^\circ\text{C}$  and charged with 7MPa of hydrogen pressure. In order to activate the sample, the reactor is evacuated for 3–4 times after charging with hydrogen. The hydrogen absorption kinetics was measured after the activation of synthesized ribbons. Fig. 3(a) shows the absorption characteristics of  $\text{Ti}_{41.5+x}\text{Zr}_{41.5-x}\text{Ni}_{17}$  ribbons synthesized at wheel speed of 45m/s. The hydrogen uptake capacity is found

to 2.15, 2.4, 2.6 and 2.7 wt% of hydrogen within 5.5hr for  $\text{Ti}_{41.5}\text{Zr}_{41.5}\text{Ni}_{17}$ ,  $\text{Ti}_{45}\text{Zr}_{38}\text{Ni}_{17}$ ,  $\text{Ti}_{53}\text{Zr}_{30}\text{Ni}_{17}$  and  $\text{Ti}_{55}\text{Zr}_{28}\text{Ni}_{17}$  i-phase ribbons respectively. The hydrogen desorption characteristics of hydrogenated ribbons were investigated through hydrogen desorption kinetics measurement performed at 350°C and 0.5 atm hydrogen pressure. Fig.3 (b) represents the representative desorption kinetics plot of nanocrystalline ribbons. From the Fig. it is clear that as we increase the Ti content desorption kinetics increases. Thus hydrogen absorption as well as desorption characteristics of synthesized nano quasicrystalline ribbons increases as we increase the content of Ti this may occur due to the formation of more finer grains which enhances the density of active grains for the interaction with hydrogen [9]. Moreover, the hydrogen uptake capacity also may increase due to the fact that the density of Ti (4.43 g/cm<sup>3</sup>) is less as compared to Zr (6.49g/cm<sup>3</sup>). Thus as the content of Ti increases and corresponding decrease in the content of Zr, the overall density of the ribbons is going to reduce and hence the overall hydrogen uptake capacity of the synthesized ribbon is increased.

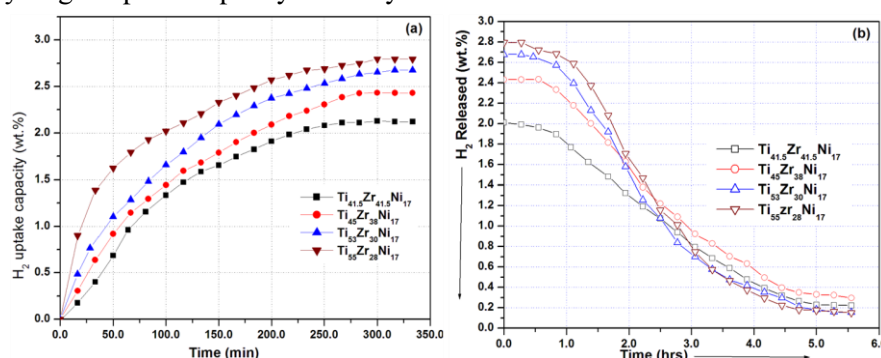


**Fig.3** (a) Hydrogen absorption kinetics plot at 320 °C & 7MPa H<sub>2</sub> pressure and (b) hydrogen desorption measurement at 350 °C & 0.5atm pressure for  $\text{Ti}_{41.5+x}\text{Zr}_{41.5-x}\text{Ni}_{17}$  ( $x=0, 3.5, 11.5$  and  $13.5$ ).

## Conclusion

We have studied the variation of the composition on structure, microstructure and their correlation for hydrogen storage characteristics of  $\text{Ti}_{41.5+x}\text{Zr}_{41.5-x}\text{Ni}_{17}$  i-phase ribbons. Nano quasi crystalline ribbons of i-phase have been synthesized through rapid solidification technique at wheel speed of 45m/s. it is found that as we increase the content of Ti and correspondingly decrease the Zr content in i-phase ribbons the formation of finer grains take place. Due to which the hydrogen uptake capacity and the kinetics of ab/desorption of hydrogen for the synthesized i-phase ribbons is increased.

## Acknowledgment

One of the authors (Dr. R. R. Shahi) would like to acknowledge the financial assistance from DST-INSPIRE Project (IFA-12-PH-43) and XRD characterization facility of CIR-MNNIT Allahabad India.

## References

- [1] Schlapbach L and Züttel 2001 *Nature* **414** 353.
- [2] Srivastava ON, Yadav TP, Shahi RR, Pandey SK, Shaz MA and Bhatnagar A 2015 *Proc. Indian Natn. Sci. Acad.* **81** 915.
- [3] Sakintuna B and Hirscher M 2007 *Int. J. of Hyd. Energy* **32** 1121.
- [4] Takasaki A and Kelton KF 2006 *Int. J. of Hyd. Energy* **31** 183.
- [5] Kelton KF, Kim WJ and Stroud RM 1997 *Appl. Phys. Lett.* **70** 24.
- [6] Stroud RM, Viano AM, Gibbons PC and Kelton KF 1996 *Appl. Phys. Lett.* **69** 20.
- [7] Lefaix H, Vermaut P, Janickovic D, Svec P, Portier R and Prima F 2009 *J Alloy Com.* **1-2** 168.
- [8] Davis JP, Majzoub EH, J.M. Simmons and Kelton KF 2000 *Mat Sci and Eng* **294-296** 104.
- [9] Shahi RR, Yadav TP, Shaz MA, Srivastava ON, Smaalen SV 2011, *Int. J hyd. Energy* **36** 592.
- [10] de Keljser Th H, Langford JI, Mittemeijer EJ, Vogels ABP 1982 *J.Appl. Cryst.* **15**, 308.
- [11] Bancel PA, Heiney PA 1985 *Phys. Rev. Letters* **54**, 2422.